

Coupled surface runoff and subsurface flow model for catchment simulations

A. C. Bixio¹, S. Orlandini², C. Paniconi³ & M. Putti¹

¹ Dipartimento di Metodi e Modelli Matematici per le Scienze Applicate, Università di Padova, Via Belzoni 7, 35131 Padova, Italy

² Dipartimento di Ingegneria, Università di Ferrara, Via Saragat 1, 44100 Ferrara, Italy

³ CRS4, Sesta Strada Ovest, Z.I. Macchiareddu, C.P. 94, 09010 Uta (Cagliari), Italy

Abstract

A distributed catchment scale numerical model for the simulation of coupled surface runoff and subsurface flow is presented. Starting from rainfall (evaporation) records, the model first determines the infiltration (exfiltration) rates in the soil, by evaluation of the soil field capacity at the specific conditions as calculated from the three-dimensional solution of the variably-saturated groundwater flow model (Richards' equation). The flow rate that remains or returns to the surface, the so called overland flow, is then routed via a diffusion wave surface runoff model based on a Muskingum-Cunge scheme with variable parameters. Both hillslope and channel flow are described, and a special algorithm is used for the simulation of pools/lakes effects on storm-flow response. The importance of including detailed subsurface flow description in catchment simulations is shown on a simple testcase characterized by the presence of a central depression.

Introduction

Simulations of catchment response to atmospheric forcing events are required by scientists and engineers who must take decisions based on hydrologic information. Although it was once sufficient to model catchment outflow, it is now often necessary to estimate distributed surface and subsurface flow characteristics as driving mechanisms for erosion, sedimentation, chemical transport and other spatially distributed effects (Abbott et al., 1986). In this sense the linkage of a distributed hydrologic model with the spatial-handling capabilities of digital elevation models (DEMs) and digital terrain models (DTMs) offers advantages associated with utilizing the full information content of spatially distributed data to analyze hydrologic processes.

Atmospheric forcing refers to precipitation intensity during storm events and potential evapotranspiration during interstorm periods. The catchment partitions this atmospheric forcing into surface runoff, groundwater flow, actual evapotranspiration, and changes in storage. Surface runoff involves different phenomena like for example hillslope and channel flow, retardation and storage effects due to pools and lakes. Groundwater flow processes include infiltration and exfiltration from the vadose zone. Typical catchment simulation models neglect exfiltration and use simple one-dimensional infiltration equations without considering horizontal flow in the subsurface. However, horizontal groundwater flow may cause exfiltration or seepage in depressed areas, as may occur, for example, in relatively flat areas characterized by the presence of shallow aquifers.

In this paper we present a physically-based distributed model for surface and subsurface simulation at catchment scale. The model couples a subsurface three-dimensional finite element module, called FLOW3D (Paniconi et al. 1994), based on the solution of the Richards' equation for variably saturated porous media, and a surface DEM-based module, SURF_ROUTE (Orlandini et al. 1996), that describes hillslope and channel flow using a diffusion-wave formulation for both phenomena. Accumulation of water in surface lakes or depressions is also implemented to account for retardation and storage effects. The two modules are coupled to give a complete description of the catchment response. The atmospheric input (in terms of precipitation and evaporation data) is partitioned into subsurface and overland flow by the FLOW3D module on the basis of the physical conditions at the surface and the soil infiltration properties. The overland flow volume is then routed by the SURF_ROUTE code returning the distribution of ponding water that will be used as boundary condition by FLOW3D. A simple preliminary example regarding a catchment characterized by a central depression shows the importance of coupling between surface and subsurface phenomena. Downslope exfiltration is shown to play a role that is at least as significant as the surface runoff.

The FLOW3D code for the solution of the subsurface problem

FLOW3D is a three-dimensional tetrahedral Finite Element model for flow in variably saturated porous media, applicable to both the unsaturated and saturated zones. It is based on the solution of Richards' equation, which may be written as (Philip, 1969):

$$\frac{\partial}{\partial x_i} \left[K_{ij} k_{rw}(S_w) \left(\frac{\partial \psi}{\partial x_j} + \zeta_j \right) \right] = \sigma(S_w) \frac{\partial \psi}{\partial t} - q_s(\psi) \quad (1)$$

where repeated indices denote summation over the three coordinate dimensions ($i, j=1,2,3$), x_i is the i th Cartesian coordinate ($x_3=z$), K_{ij} is the saturated hydraulic conductivity tensor, $k_{rw}(S_w)$ is the relative hydraulic conductivity function, $S_w(\psi)$ is the water saturation, ψ is the pressure head, $\zeta_1 = \zeta_2 = 0$, $\zeta_3 = 1$, σ is the general storage term, t is time, and q_s represents distributed source or sink terms (volumetric flow rate per unit volume). The characteristic relationships $k_{rw}(S_w)$ can be specified in FLOW3D using the van Genuchten and Nielsen (1985), Brooks and Corey (1964) or Huyakorn et al. (1984) models.

Equation (1) is highly nonlinear due to the pressure head dependencies in the storage and conductivity terms, and is linearized in the code using either Picard or Newton iteration (Paniconi and Putti, 1994). Tetrahedral elements and linear basis functions are used for the discretization in space, and a weighted finite difference scheme is used for the discretization in time.

The code handles temporally and spatially variable boundary conditions, including seepage faces and atmospheric inputs, heterogeneous material properties and hydraulic characteristics, and various expressions to describe the moisture content-pressure head and relative conductivity-pressure head relationships (Paniconi et al., 1994).

For the treatment of the atmospheric boundary conditions, the input flux values are considered "potential" rainfall or evaporation rates, and the "actual" rates, which depend on the prevailing flux and pressure head values at the surface, are dynamically calculated by the code during the simulation. Overland flow, defined as the flow rate that is present at surface and that can be routed via the surface model, is calculated at every time step on the basis of potential and actual fluxes.

Automatic switching of surface boundary conditions from a specified flux (Neumann) to a constant head (Dirichlet) boundary condition, and vice versa, is implemented to correctly reproduce the physical phenomena occurring at the surface. This automatic switching can be more easily described by means of a few characteristic examples. In case of precipitation, if a surface node becomes saturated because of infiltration excess, the fraction of precipitation that does not infiltrate and remains at the surface becomes the overland flow to be routed via the surface module. The boundary conditions in this case switch from Neumann (atmospheric-controlled) to Dirichlet (soil-controlled) type because infiltration is now driven by the fraction of the precipitation flux that cannot infiltrate and that remains at the surface (ponding head). If precipitation intensity decreases, so that the magnitude of actual (computed) flux across the soil surface exceeds the magnitude of the atmospheric flux, the boundary condition switches back to a Neumann type. If a surface node becomes saturated because of saturation excess, and there is an upward flux across the soil surface (return flow), the overland flow is calculated as the sum of precipitation and return flux. The entire amount of water that remains at the surface or exfiltrates from the subsurface is then transferred for routing to a DEM-based surface runoff module. This code, as explained in more details in the next section, will return the routed ponding head distribution to be used where necessary as Dirichlet (soil-controlled) boundary condition in FLOW3D.

The DEM-based SURF_ROUTE model for surface runoff in hillslopes, channels and lakes

The surface hydrologic response of a catchment is considered as determined by the two processes of hillslope and channel transport, operating across all the hillslopes and stream channels forming a watershed, by the storage and retardation effects of pools or lakes and by the effects of infiltration/evapotranspiration and exfiltration from subsurface soils.

Hillslope processes

We assume that hillslope flow concentrates in defined rills or rivulets that form because of topographic irregularities or differences in soil erodibility and that deepen and widen during the runoff event as function of slope, runoff characteristics and soil erodibility. To minimize the computational effort and economize on the number of model parameters the rill formation are lumped at the DEM elemental scale into a single conceptual channel. The drainage system topography and composition are described by extracting automatically a conceptual drainage network from the catchment DEM. Each elemental hillslope rill and network channel is assumed to have bed slope and length that depend on location within the extracted transport network, and rectangular cross section whose width varies dynamically with discharge according to the scaling properties of stream geometry as described by the “at-a-station” and “downstream” relationships first introduced by Leopold and Maddock (1953). Distinction between hillslope and channel flow is based on the “constant critical support area” concept as described by Montgomery and Foufoula-Georgiou (1993). Rill flow is assumed to occur for all those cells for which the upstream drainage area A does not exceed the constant threshold value A^* , while channel flow is assumed to occur for all those cells for which A equals or exceeds A^* .

A routing scheme developed on the basis of the Muskingum-Cunge method with variable parameters is used to describe both hillslope rill and network channel flows, with different distributions of the Gauckler-Strickler roughness coefficients to take into account the different processes that characterize the two physical phenomena (Orlandini & Rosso, 1998). The model routes surface runoff downstream from the uppermost DEM cell in the basin to the outlet, following the previous determined drainage network. A given grid cell will receive water from its upslope neighbor and discharge it to its downslope neighbor, with the lateral inflow rate $q_L (L^2T^{-1})$ at any catchment cell given by:

$$q_L = q\Delta x\Delta y / \Delta s$$

where $q (LT^{-1})$ is the local contribution to surface runoff, Δx and Δy are the cell sizes, and Δs is the channel length within the cell.

Inflow hydrographs and lateral inflows q_L are routed into each individual channel via a convection diffusion flow equation:

$$\frac{\partial Q}{\partial t} + c_k \frac{\partial Q}{\partial s} = D_h \frac{\partial^2 Q}{\partial s^2} + c_k q_L \quad (2)$$

where Q is the discharge along the channel coordinate s , c_k is the cinematic wave celerity, and D_h the hydraulic diffusivity, discretized by the Muskingum-Cunge scheme:

$$Q_{i+1}^{k+1} = C_1 Q_i^{k+1} + C_2 Q_i^k + C_3 Q_{i+1}^k + C_4 q_{Li+1}^k \quad (3)$$

where Q_{i+1}^{k+1} is discharge at network point $(i+1)\Delta s$ and time $(k+1)\Delta t$ and q_{Li+1}^k is the lateral inflow rate at the $(i+1)st$ space interval and time $k\Delta t$, and the routing coefficients C_i depend on c_k , on the temporal interval Δt , on the channel length Δs , and on the numerical discretization.

Once the in and out discharge at each cell is determined, the cell water depth, or ponding head, h , can be calculated with simple mass balance considerations.

Modeling the topographic depressions

Isolated topographic depressions (“pits”) in the catchment DEM can be attributed to the presence of pools or lakes, or can be interpreted as erroneous or missing data. Depressions cannot be handled by automatic drainage network extraction procedures, and depitting techniques are generally used to modify the elevation values and to regularize the DEM. These depitting schemes are necessary and sufficient to correct DEM errors, and can be also used in steep basins, where the flow is mainly driven by slope and the artificial modification of topography in some points does not significantly change surface flow patterns. However, when depressions play an important role in the formation of surface and subsurface fluxes these procedures introduce inconsistent flow directions and do not correctly reproduce the storage and retardation effects of pools and lakes on the catchment response. This typically happens in relatively flat areas where flow patterns are strongly influenced by small slope changes.

In the present paper topographic depressions are treated as follows. Initially the location of the pits is identified from the DEM and from prior field information. A “lake boundary-following” procedure (Mackay and Band, 1998) is employed to isolate and correct for potential breakdown in the subsequent drainage network extraction process. By this procedure, each cell along the boundary of the pit (also called “buffer cells”) acts as a depression point for all the catchment cells draining into the pit. To ensure correct flow paths in the area, the drainage direction in all the buffer cells is forced to form a circulation path that drains into a single cell (the lake outlet cell). A flow path

algorithm, in combination with a “slope tolerance” based correction procedure to account for the remaining erroneous depressions, is then applied to the modified DEM that excludes the central cells of the depression. The storage and retardation effects of the pit are accounted for by transferring with infinite celerity all the water drained by the buffer cells to the outlet, which is now considered as a reservoir. All the geometrical and physical characteristics of the depression are then attributed to this cell. Outflow from this cell is calculated by solving, by a level pool routing procedure, the continuity equation for the reservoir:

$$\frac{\partial V}{\partial t} = I(t) - O(h) \quad (4)$$

where V is the storage volume of the reservoir, I and O are the incoming and outgoing discharges, functions of time t and of water level in the reservoir h , respectively. The reservoir water level thus determined is assigned to all the lake cells and used in FLOW3D as ponding head, while the discharge from the reservoir is the outgoing flux at the cell to be used in SURF_ROUTE.

Coupling the surface and subsurface models

The surface routing and subsurface flow phenomena are physically coupled: in fact, the overland flow rate is affected by the precipitation (evaporation) and infiltration (exfiltration) rates. In turn, infiltration (exfiltration) is affected by precipitation (evaporation) and the ponding head resulting from surface routing. The coupled mathematical model can be written as:

$$\frac{\partial}{\partial x_i} \left[K_{ij} k_{rw} (S_w) \left(\frac{\partial \psi}{\partial x_j} + \zeta_j \right) \right] = \sigma(S_w) \frac{\partial \psi}{\partial t} - q_s(h) \quad (5)$$

$$\frac{\partial Q(h)}{\partial t} + c_k \frac{\partial Q(h)}{\partial s} = D_h \frac{\partial^2 Q(h)}{\partial s^2} + c_k q_L(h, \psi) \quad (6)$$

This system of PDEs is solved simultaneously for the unknown vector (Q, ψ) or (h, ψ) using the FLOW3D and SURF_ROUTE models previously described.

Coupling is in general nonlinear due to the dependence of q_s on the ponding head and the nonlinear dependence of q_L on ψ . However, the explicit in time nature of the Muskingum-Cunge discretization scheme allows the construction of the following non-iterative algorithm for the solution of the (5) and (6):

for $t_k=0$ to t_{max} with step Δt :

- set $t^{k+1} = t^k + \Delta t$
- solve (6) using q_L^k as input to the SURF_ROUTE model, obtaining the distribution of ponding head h^{k+1}
- use h^{k+1} and precipitation (evaporation) input at time t^{k+1} to set up boundary conditions for FLOW3D and solve (5) for ψ^{k+1}
- calculate (again with FLOW3D) the overland flux q_L^{k+1} using ψ^{k+1} and atmospheric inputs.

The algorithm needs to be initialized by setting an initial condition in terms of q_L for equation (6). If this condition is not known a priori, it is calculated by means of an

initial run of FLOW3D that will evaluate a first guess for the overland flow based on the actual atmospheric input.

Application

The coupled surface-subsurface model has been tested on the hypothetical basin of Figure 1. The basin is formed by 6 x 11 surface cells 50 x 50 m wide, with elevations varying between 15 and 10 m m.s.l., and is characterized by a depression in its central part with a minimum elevation of 11 m m.s.l..

During drainage network extraction the 9 central cells of the depression have been eliminated from the surface DEM. In the surrounding cells ("buffer cells") the flow direction has been imposed so that the water is drained by the depression towards the reservoir, indicated by the letter R in Figure 1, in which the geometrical characteristics of the whole depression are concentrated. Water is allowed to flow out from the reservoir when the level raises above 14 m, which is the real elevation of the lowest cell surrounding the depression.

For the runoff simulation, no channel flow has been allowed, assigning a high value to the threshold area A^* . A constant value of $10 \text{ m}^{1/3} \text{ s}^{-1}$ has been imposed to the Gauckler-Strickler surface roughness coefficient. The underlying aquifer is assumed to have a constant thickness of 10 m, and is divided into two parallel 5 m thick layers, characterized by hydraulic conductivity values of 10^{-4} and 10^{-5} m/s. Hydrostatic distribution of pressure head has been assigned as boundary condition along the vertical boundaries of the 3D domain. Initial conditions of zero pressure head at the surface is imposed. The catchment is subjected to a constant and homogeneous precipitation intensity of 6.0×10^{-5} m/s has been imposed.

Figure 2 illustrates the infiltration (positive) and exfiltration (negative) fluxes as calculated by the coupled code at different simulation times. The corresponding distribution of water head at the surface (ponding head) is reported in Figure 3.

It can be observed that water infiltrates everywhere in the basin except than in correspondence of the depression and of the outlet cell. These depressed areas are subjected to downslope exfiltration of water. Exfiltration in the depression continues even when a relevant ponding head (2.8 m) is present, because of the higher phreatic level in the cells surrounding. A higher ponding head in the lake would be necessary to switch the subsurface flow from exfiltration to head-controlled infiltration under the lake.

12	11	10	11	12	13
12	12	12	12	12	13
13	13	13	13	13	14
14	14	14	14	14	15
14	13	13	13	14	15
13	12	12	12	13	14
13	12	11	12	13	14
13	12	12	12	13	14
14	14	14	14	14	15
14	14	14	14	14	15
15	15	15	15	15	15

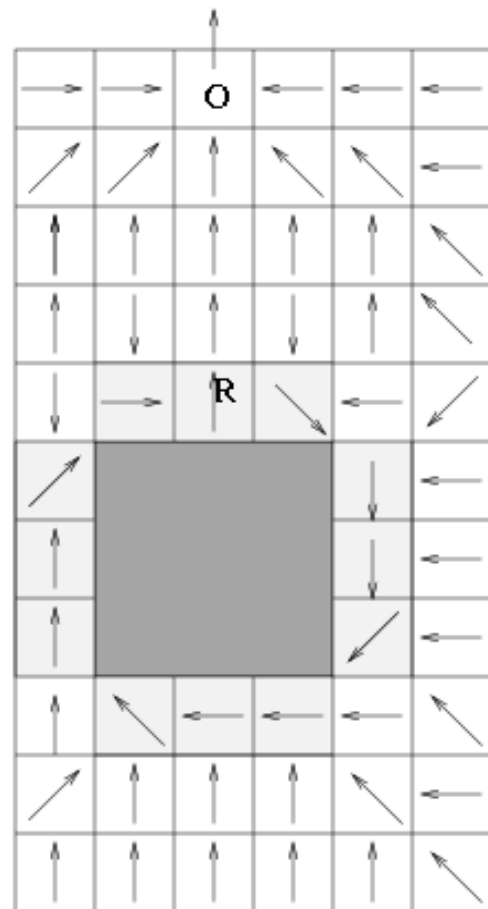


Figure 1. The catchment DEM with elevations (m m.s.l.) (left) and a schematized representation of the catchment with flow paths as calculated by the “depitting” procedure (right). The interior area of the depression is displayed in dark grey, the buffer cells with forced flow directions in light grey, the reservoir cell is identified by the letter “R”, while “O” is the outlet cell.

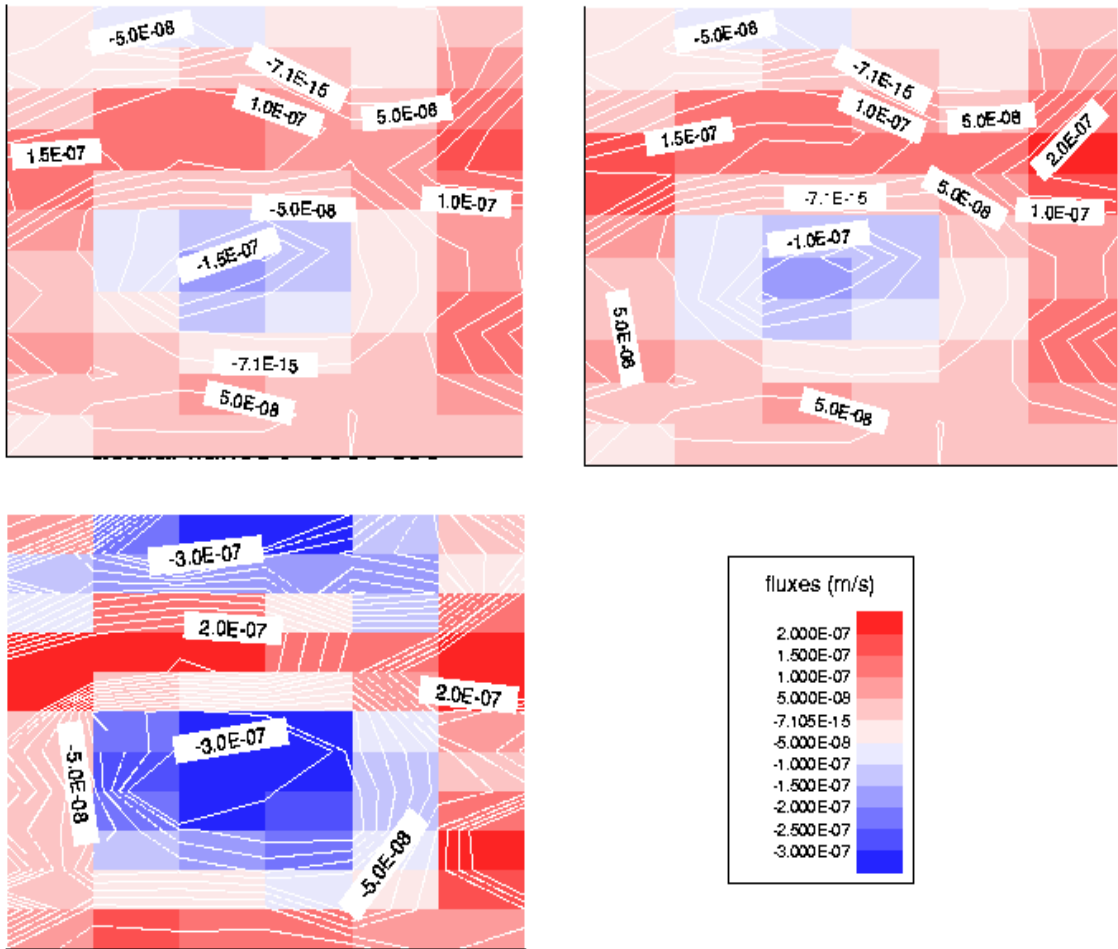


Figure 2: Infiltration (positive) and exfiltration (negative) rates at surface calculated at simulation times 40 min (top left), 170 min (top right) and 210 min (lower left).

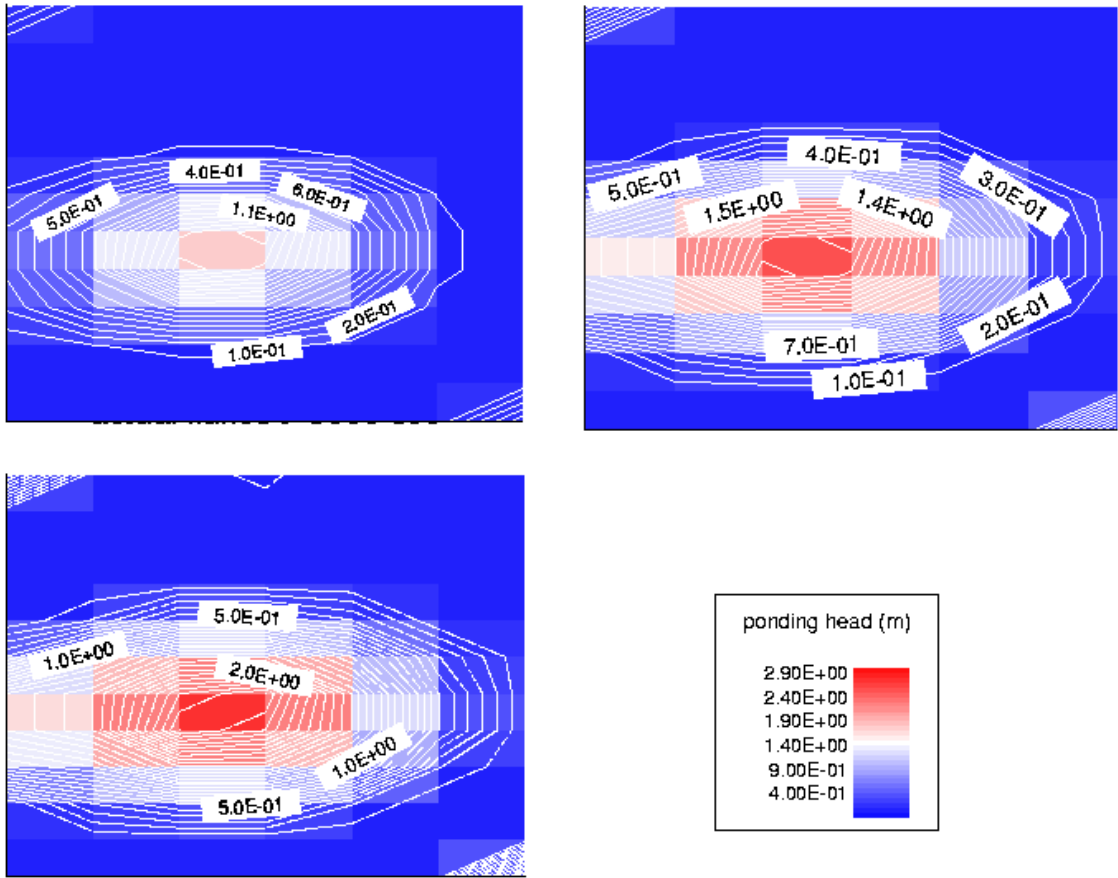


Figure 3: Ponding head at the surface calculated at simulation times 40 min (top left), 170 min (top right) and 210 min (lower left).

Acknowledgement

This research was supported by EC through the Inco-Copernicus program (Contract No. ERBIC15CT960211).

References

- Abbott, M.B., Bathrust, J.C., Cunge, J.A., O'Connell, P.E., 1986. An introduction to the European Hydrological System, Systeme Hydrologique Europeen, "SHE",1, History and philosophy of a physically-based, distributed modeling system. J. Hydrol., 87,45-59.
- Brooks, R.H. & Corey, A.T., 1964. Hydraulic Properties of porous media. Hydrology Paper n. 3, Colorado State Univ., Fort Collins, Colorado.
- Huyakorn, P.S., Thomas, S.D. & Thompson, B.M., 1984. Techniques for making finite elements competitive in modeling flow in variably saturated porous media Water Resources Research, vol.20[8], 1099-1115.

- Leopold, L.B. & Maddock, T., 1953. The hydraulic geometry of stream channels and some physiographic implications. U.S. Geol. Surv. Prof. Pap. 1302.
- Mackay, D.S. & Band, L.E., 1998. Extraction and representation of nested catchment areas from digital elevation models in lake-dominated topography. *Water Resources Research*, vol. 34[8], 897-901.
- Montgomery, D.R. & Foufoula-Georgiou, 1993. Channel network source representation using digital elevation models. *Water Resources Research*, vol. 29[12], 3925-3934.
- Orlandini, S., Mancini, M., Paniconi, C. and Rosso, R., 1996. Local contribution to infiltration excess runoff for a conceptual catchment scale model. *Water Resources Research*, vol. 32[7], 2003-2012.
- Orlandini, S. & Rosso, R., 1998. Parametrization of stream channel geometry in the distributed modeling of catchment dynamics. *Water Resources Research*, vol. 34[8], 1971-1985.
- Paniconi, C., Ferraris, S., Putti, M., Pini, G. & Gambolati, G., 1994. Three-Dimensional Codes for Simulating Groundwater Contamination: FLOW3D, Flow in Saturated and Unsaturated Porous media. In: editor Paolo Zannetti, Proc. Envirosoft 94, CMP, Southampton UK, 149-156.
- Paniconi, C. & Putti, M., 1994. A comparison of Picard and Newton iteration in the numerical solution of multi-dimensional variably saturated flow problems. *Water Resources Research*, vol. 30[12], 3357-3374.
- Philip, J.R., 1969. Theory of infiltration. *Adv. Hydrosoci.*, 5, 215-296.
- van Genuchten, M.T. Nielsen, D.R., 1985. On describing and predicting the hydraulic properties of unsaturated soils. *Ann. Geophys.*, 3[5], 615-628.